Results in Engineering 13 (2022) 100366

Contents lists available at ScienceDirect

Results in Engineering

journal homepage: www.sciencedirect.com/journal/results-in-engineering

A study of the mesh effect on a rocket plume simulation

Federico N. Ramírez [a], Mara S. Escarti-Guillem [a,b], Luis M. García-Raffi [a], Sergio Hoyas [a,*]

[a] Instituto Universitario de Matematica Pura y Aplicada, Universitat Politècnica de València, 46022, Valencia, Spain
[b] Comet Ingeniería, Convento Carmelitas, 2, 46010, Valencia, Spain

ARTICLE INFO

Keywords:
Mesh
Rocket launch
Supersonic jet
OpenFOAM

ABSTRACT

The use of reliable CFD models for the simulation of spacecraft launch is crucial due to the complexity of obtaining experimental data. The validity of the results depends on the numerical schemes used and the mesh. In this paper two CFD simulations of a supersonic jet have been conducted using OpenFOAM. Two different mesh types have been compared, hexaedral and polyhedral. Our calculations show that the former is more accurate and faster than the latter. Moreover, the minimum required element has been estimated to be 50 cells/diameter.

1. Introduction

The study of the phenomena that occurs during a rocket launch is extremely complicated due to the extreme conditions that are reached. Because of this, the amount of experimental data and the existing empirical correlations are limited. Therefore, a suitable CFD methodology to study the flow behaviour in these situations is required. The exhaust gas rocket plume is the main source of noise generation, being the most studied region of the flow [5]. This work is the first step towards a rocket launch aero-acoustic study.

In this paper, we consider the influence of the type of element used on the quality of the results and the computational cost. We also estimate the element size needed to obtain an adequate solution.

2. Methodology

Every simulation presented here has been done in OpenFOAM v1912 software. OpenFOAM [10] is a widely-used open source software with proven reliability. As usual in CFD, it uses the finite volume method for spatial discretization. About turbulence, Reynolds-Averaged Navier--Stokes turbulence modelling (RANS) has been applied.

Given the characteristics of the case studied, the rhoPimpleCentralFoam [6] solver was used due to its good performance in supersonic flow. It is a solver that combines the PIMPLE algorithm with the use of the upwind-central discretization schemes of Kurganov and Tadmor [7, 8].

First-order Upwind scheme is used for the convective terms of the variables associated with turbulence and second-order Gauss Linear for the rest of the variables and the gradients, switching to Upwind in the large gradient regions. Second-order Gauss Linear is selected for Laplacian terms, and second-order Van Leer is employed as interpolation scheme.

The Standard $k-\varepsilon$ scheme as described in Refs. [9,11] is used to model the unresolved turbulence. Standard $k-\varepsilon$ presents a good performance in free-shear flows. As in Ref. [4], the value of the coefficient C_1 has been modified from 1.44 to 1.6. This change improves the predictions on round jet modelling [4].

The computational volume consists of a 0.4 × 0.4 × 1.6 m hexahedron and the outflow section is a 0.2 m diameter circumference. We have produced two different meshes to study the influence of the mesh type. First, a fully hexahedral mesh, generated through snappyHexMesh. Second, we computed a polyhedral mesh through the polyDualMesh tool from a tetrahedral one. Both meshes are shown in Fig. 1. They have an element size of 0.4 mm in the jet exit region. As a result, the hexahedral mesh is composed of 1 200 000 cells, while the polyhedral mesh contains 750 000 cells.

Regarding boundary conditions, the nozzle is defined as an inlet. The rest of the surfaces of the rocket awe modelled as a wall. The external faces of the volume were defined as an outlet. The values of pressure, temperature and velocity used for these boundaries are the ones used in Ref. [3].

Finally, a mesh independence study is performed. Since RANS simulations are relatively Reynolds independent in free flow zones, the result of this study can be extrapolated to a simulation performed with a real geometry. Table 1 shows the most representative data of the hexahedral meshes used for this particular analysis. As for the polyhedral meshes, the element size in the jet zone has been modified to obtain two meshes, with half and triple the number of elements respectively.

---

* Corresponding author.
E-mail address: serhocal@upvnet.upv.es (S. Hoyas).

https://doi.org/10.1016/j.rineng.2022.100366
Received 19 December 2021; Received in revised form 28 January 2022; Accepted 7 February 2022

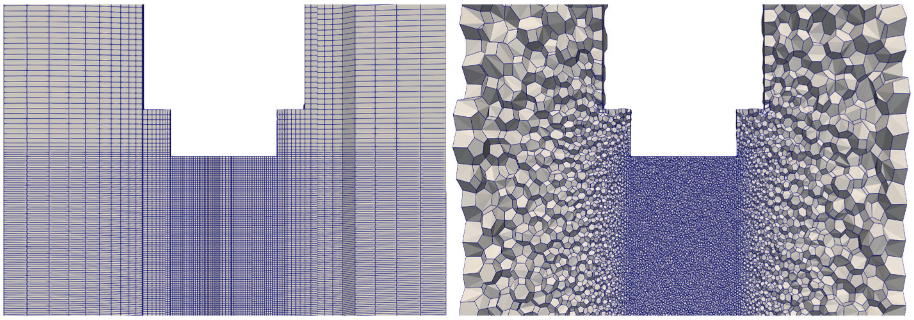

Fig. 1. Hexahedral mesh (left) and polyhedral mesh (right).

Table 1
Mesh independence summary.

	Min. size	Number of cells	Cells/diameter
Mesh1	5 mm	600 000	40
Mesh2	4 mm	1 200 000	50
Mesh3	2.5 mm	4 000 000	80
Mesh4	2 mm	6 000 000	100

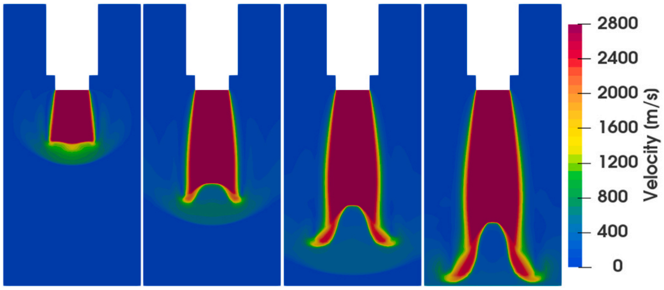

Fig. 2. Velocity field for the hexahedral mesh. From left to right, t = 0.4 ms, t = 0.8 ms, t = 1.2 ms and t = 1.6 ms.

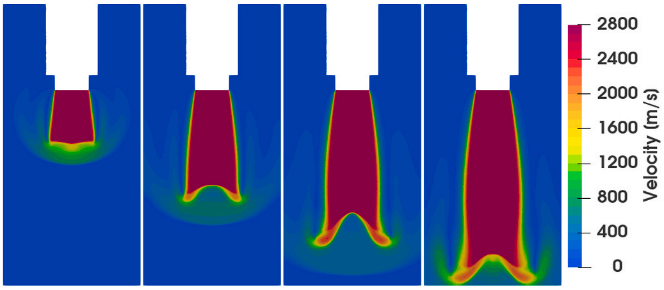

Fig. 3. Velocity field for the polyhedral mesh. From left to right, t = 0.4 ms, t = 0.8 ms, t = 1.2 ms and t = 1.6 ms.

3. Results and discussion

Figs. 2 and 3 show the velocity contours corresponding to the hexahedral and polyhedral meshes Four different time instants are shown. As expected for a supersonic jet, a normal shock wave appears as the flow develops. It can be seen that this wave is larger in the case of the hexahedral mesh causing the jet development to differ between the two cases. This may be due to the higher diffusion of the polyhedral elements since the faces are not aligned with the flow direction. Similar results have been found in the literature, such as [1] which demonstrates the higher accuracy of hexahedral elements to correctly capture shock waves, or [2] where the differences found in the polyhedral mesh are attributed to viscous effects.

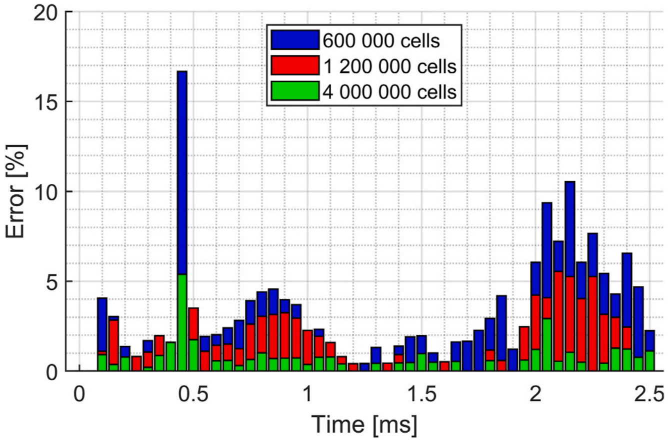

Fig. 4. Relative error in hexahedral meshes with respect to the most refined one (6 000 000 cells).

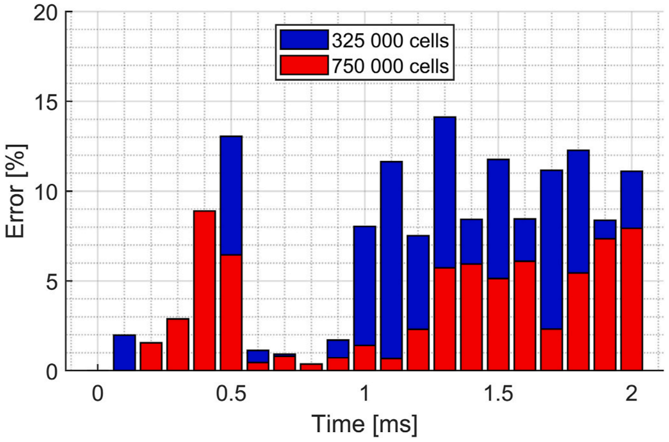

Fig. 5. Relative error in polyhedral meshes with respect to the most refined one (2 250 000 cells).

About the computational cost, the difference is significant. The simulation of the hexahedral mesh has taken 10.3 h, while the one of the polyhedral mesh has taken 42.8 h. Both simulations have been performed on two Intel Xeon Gold 6148 CPUs using 64 cores. This difference can be explained by two reasons. On the one hand, even with fewer elements, the number of faces of each cell is larger in the case of the polyhedral mesh, so the number of operations per cell increases. On the other hand, when the polyhedral mesh is created by the described process, small elements are generated near the rocket geometry. These elements limit the maximum time step.

The mesh independence study is summarised in Figs. 4 and 5. Here the error is defined as the relative difference in the jet front advance with respect to the most refined mesh. For the hexahedral meshes it can be seen how, in general, the error remains below 10% for the mesh of 1 200 000 cells, and always below 5% for the mesh of 4 000 000 cells. Furthermore, the average error is 3%, 1.9% and 0.55% for the three meshes respectively. For polyhedral meshes the average error is 6.45% and 3.45% respectively.

4. Conclusions

In conclusion, the hexahedral mesh seems to be the right choice for supersonic jet simulation by reducing the computational cost and avoiding the higher diffusion related to the non-alignment between the flow and the cell faces.

As for the cell size, it has been found that 50 cells/diameter seems to be a suitable size for this type of simulations, while from 80 cells/diameter onwards the error committed starts to be negligible.

Credit author statement

Conceptualization, S.H. and L.G-R.; methodology, S.H., M.E-G. and L.G-R.; software, F.N.R.; validation, S.H., M.E-G. and L.G-R.; formal analysis, F.N.R and M.E-G.; resources, S.H.; writing—original draft preparation, F.N.R and M.E-G.; writing—review and editing, S.H., L.G-R.; supervision, S.H. and L.G-R.; funding acquisition, S.H., and L.G-R. All authors have read and agreed to the published version of the manuscript.

Declaration of competing interest

The authors declare that they have no known competing financial interests or personal relationships that could have appeared to influence the work reported in this paper.

Acknowledgment

FNR is currently at CMT-Motores Térmicos, Universitat Politècnica de València. The work was supported by the Spanish Ministry of Science and Innovation (MICINN)/FEDER [grant numbers DIN2019-010877, RTI2018-102256-B-100].

References

[1] G. Bono, A.M. Awruch, Numerical Study between Structured and Unstructured Meshes for Euler and Navier-Stokes Equations, 2007.
[2] C. Brehm, Emre Sozer, Shayan Moini-Yekta, Jeffrey Housman, Cetin Kiris, Michael Barad, Vu Bruce, Parlier Christopher, Computational prediction of pressure and thermal environments in the flame trench with launch vehicles, in: 31st AIAA Applied Aerodynamics Conference, 2013.
[3] M.S. Escarti-Guillem, S. Hoyas, L.M. García-Raffi, Rocket plume urans simulation using openfoam, Result. Eng. 4 (2019) 100056.
[4] S. Hoyas, J. Pastor, D. Khuong, J. Mompó-Laborda, F. Ravet, Evaluation of the eulerian-Lagrangian spray atomisation (elsa) in spray simulations, Int. J. Veh. Syst. Model. Test. 6 (2011) 187–201.
[5] C. Jiang, T. Han, Z. Gao, C.H. Lee, A review of impinging jets during rocket launching, Prog. Aero. Sci. 109 (2019) 100547.
[6] M. Kraposhin, A. Bovtrikova, S. Strijhak, Adaptation of kurganov-tadmor numerical scheme for applying in combination with the piso method in numerical simulation of flows in a wide range of mach numbers, 4th International Young Scientist Conference on Computational Science, Procedia Comput. Sci. 66 (2015) 43–52.
[7] A. Kurganov, S. Noelle, G. Petrova, Semidiscrete central-upwind schemes for hyperbolic conservation laws and Hamilton–Jacobi equations, SIAM J. Sci. Comput. 23 (2001) 707–740.
[8] A. Kurganov, E. Tadmor, New high-resolution central schemes for nonlinear conservation laws and convection–diffusion equations, J. Comput. Phys. 160 (2000) 241–282.
[9] B. Launder, D. Spalding, The numerical computation of turbulent flows, Comput. Methods Appl. Mech. Eng. 3 (1974) 269–289.
[10] OpenCFD, Openfoam web, URL: https://www.openfoam.com, 2021.
[11] S.H.E. Tahry, k-epsilon equation for compressible reciprocating engine flows, J. Energy 7 (1983) 345–353.